Supplemental Information

Loss and gain of *Drosophila* TDP-43 impair synaptic efficacy and motor control leading to age-related neurodegeneration by loss-of-function phenotypes

Danielle C. Diaper[1,7], Yoshitsugu Adachi[1,7], Ben Sutcliffe[2], Dickon M. Humphrey[1], Christopher J. H. Elliott[3], Alan Stepto[1], Zoe N. Ludlow[1], Lies Vanden Broeck[4], Patrick Callaerts[4], Bart Dermaut[4,5], Ammar Al-Chalabi[6], Christopher E. Shaw[6], Iain M. Robinson[2] & Frank Hirth[1,*]

[1]MRC Centre for Neurodegeneration Research, King's College London, Department of Neuroscience, Institute of Psychiatry, London/UK;

[2]Peninsula College of Medicine and Dentistry, Universities of Exeter and Plymouth, Plymouth/UK;

[3]Department of Biology, University of York, York/UK;

[4]Laboratory of Behavioural & Developmental Genetics, Centre for Human Genetics, University of Leuven & VIB Centre for the Biology of Disease, Leuven/Belgium;

[5]INSERM U744, Pasteur Institute of Lille, University of Lille North of France, Lille/France.

[6]MRC Centre for Neurodegeneration Research, King's College London, Department of Clinical Neuroscience, Institute of Psychiatry, London/UK;

[7]*these authors contributed equally to this work*

*Correspondence to Frank.Hirth@kcl.ac.uk

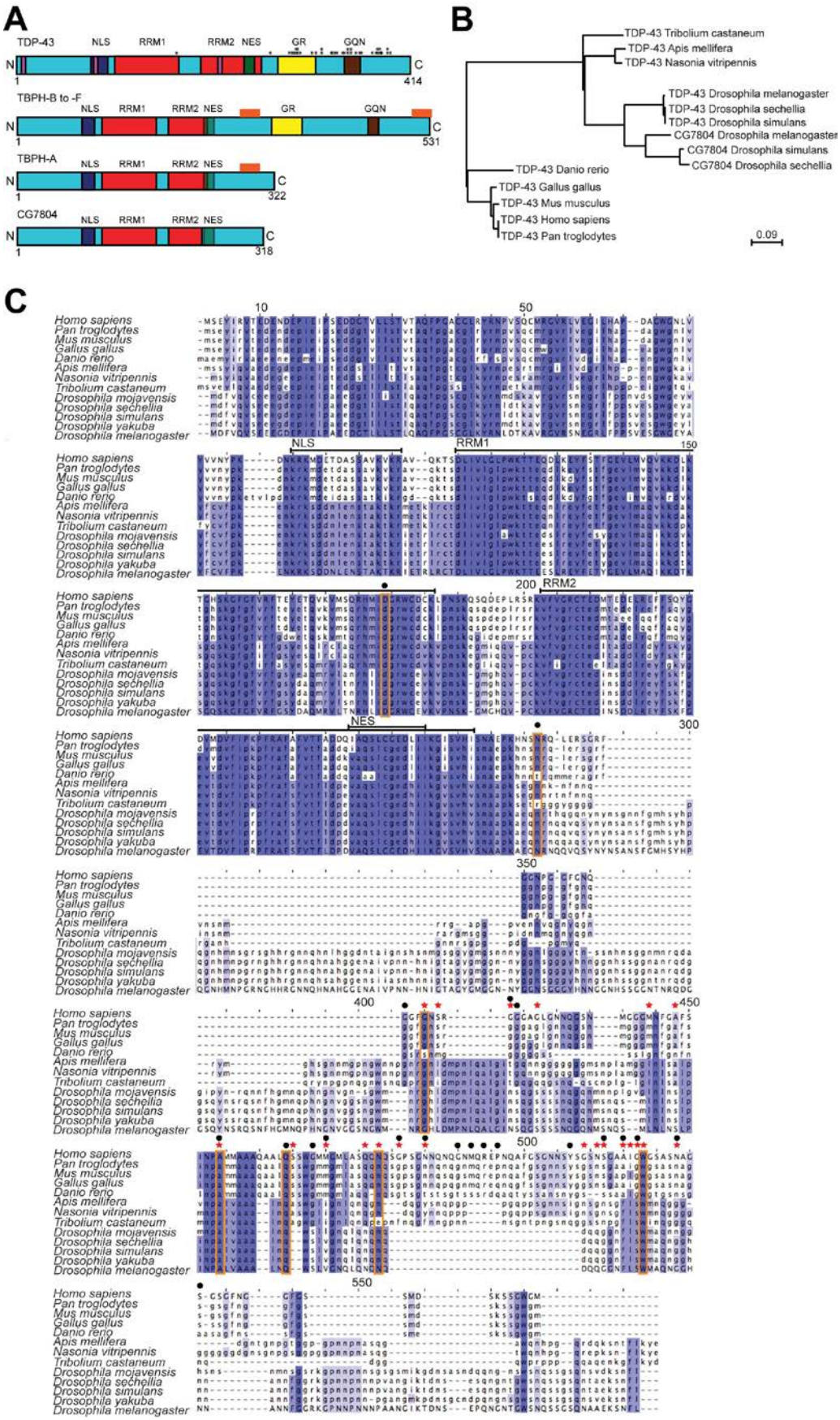

Figure S1. TAR DNA Binding Protein Homologue (TBPH) encodes the *Drosophila* homologue of TDP-43. (**A**) Human TDP-43 is 414 amino acids in length and contains two RRM domains (red), a

nuclear localization signal (NLS, blue), nuclear export signal (NES, green), a glycine rich (GR, yellow) and glycine, glutamine and asparagine (GQN, brown) domain. There are also 3 predicated caspase3 cleavage sites (pink bar). The asterisks indicate identified missense mutation in ALS. TBPH isoforms -B to -F are 531 amino acids long and contain similar domains to the human protein, however, TBPH does not contain any predicted caspase3 cleavage sites. The horizontal orange bars indicate the regions used to generate the rabbit anti-TBPH antibody. The TBPH-A isoform, which is 322 amino acids long, lacks the C-terminus region and is similar to the 318 amino acid-long CG7804 gene. (**B**) Phylogenetic tree derived from a pairwise alignment of various TDP-43 and CG7804 protein sequences. A fast minimum evolution analysis was carried out on a pairwise multiple sequence alignment of selected TDP-43 and CG7804 proteins. The line length indicates the genetic distance, which is a measure based on the minimum number of substitutions required to convert one sequence into another. (**C**) A multiple protein alignment using ClustalW 2 details the homology between TBPH and TDP-43 from a range of other eukaryotes and *Drosophila* species. The N-terminal region of TDP-43, which contains the RNA recognition motif (RRM) domains, is highly conserved throughout the species. The blue shading represents the degree of homology between the different species; dark blue indicates highly conserved amino acids, whereas light blue indicates partially conserved sites (similarity). No shading indicates that there is no homology or similarity at that site. Red stars indicate FALS mutation sites and black circles, SALS. The orange vertical bars identify ALS-linked TDP-43 mutations at sites that are conserved in the long TBPH isoform. Note: The numbered amino acid position (top row) takes into account all gap positions and does not reflect the actual amino acid position within the protein.

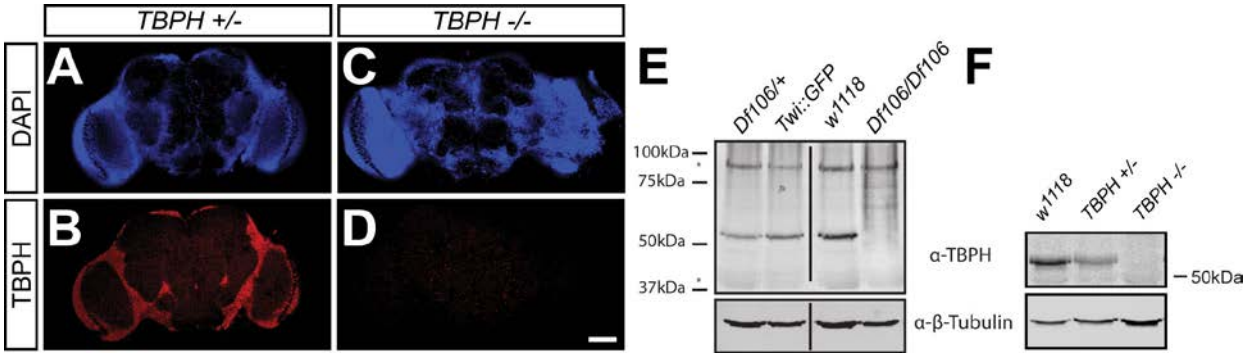

Figure S2. A polyclonal TBPH antibody specifically recognizes a 58kDa protein. The specificity of the anti-TBPH antibody was confirmed via immunohistological staining of adult brains of *TBPH-/-* null mutants and heterozygous *TBPH+/-* controls. (**A-D**) Adult heterozygous deletion mutants show TBPH expression throughout the adult brain, whereas TBPH null flies do not show any fluorescent signal using the anti-TBPH antibody. Images are single z-slices with 1um step size. (**E**) A Western blot of protein extracts from 20 embryos of heterozygous *Df(2R)106* (*Df(2R)106/+*), a control *TwiGAL4>GFP* that was used to select homozygous deficiency embryos, w^{1118} and homozygous *Df(2R)106* which shows that the anti-TBPH antibody detects a specific band at 58kDa in the controls that is not present in the homozygous *Df(2R)106* embryos. The Df(2R)106 deficiency line has a large deletion in 2R which includes the entire TBPH loci. The asterisks indicate non-specific bands. The vertical bar indicates removal of part of the image, however, all samples were run on the same gel. (**F**) Protein extracts from 6 adult heads of *TBPH-/-* flies also lack a band at 58kDa when probed with the anti-TBPH antibody. Scale bar: 50 µm.

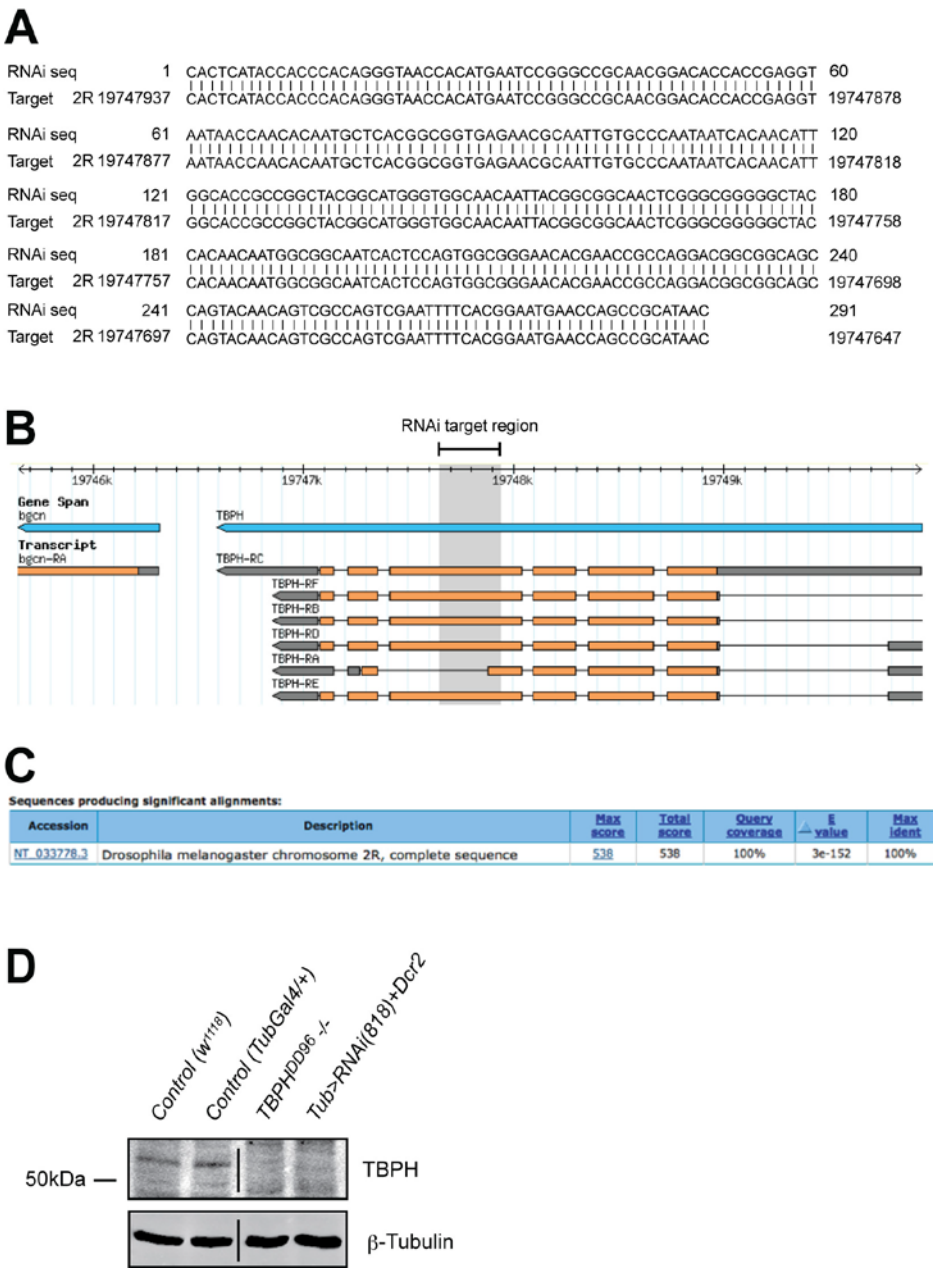

Figure S3. TBPH-RNAi effectively knocks down TBPH protein expression and has no predicted off-targets. (**A**) The TBPH-RNAi construct and target sequence. (**B**) The TBPH-RNAi target region covers all known TBPH isoforms. (**C**) A BLAST search using the TBPH-RNAi sequence produces only 1 significant alignment, which is in the TBPH locus. (**D**) Western blot analysis shows that activation of TBPH-RNAi and Dcr2 by the ubiquitous driver Tubulin-Gal4 leads to effective knock down of TBPH protein expression, comparable to the TBPH -/- mutant.

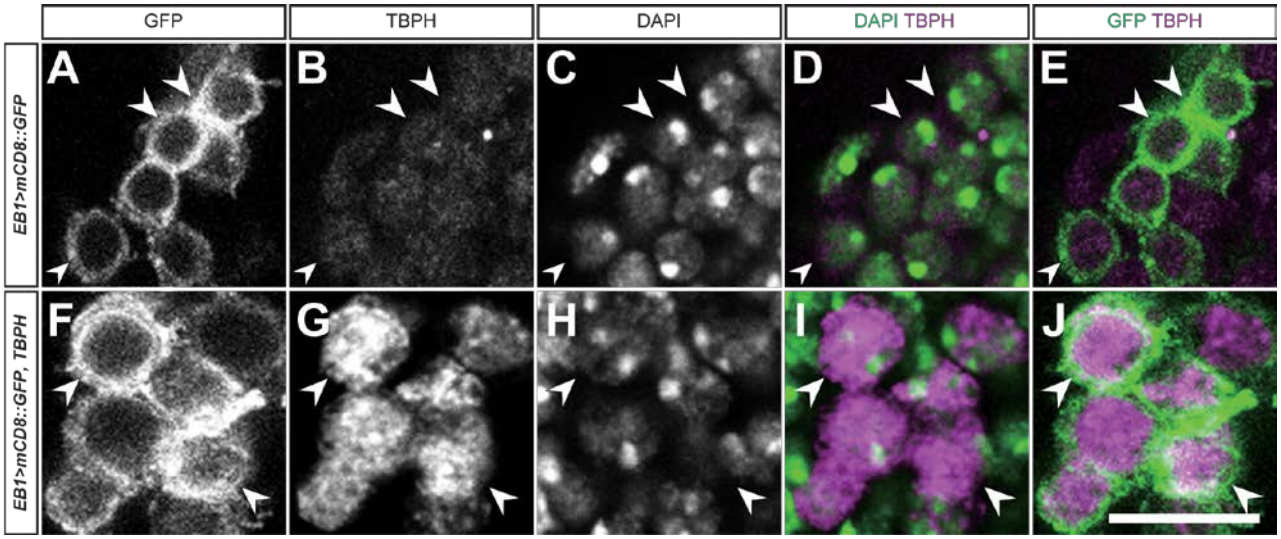

Figure S4. Gain of TBPH leads to protein accumulation in both nucleus and cytoplasm. (**A-E**) Control 5-day old *EB1>mCD8::GFP* brain shows endogenous TBPH expression in upper motor neurons. **(A-C)** Single channels of GFP **(A)**, TBPH **(B)**, and DAPI **(C)** are shown. **(D)** Merged image of **B** and **C**. TBPH is expressed in the nucleus, as indicated by its co-localisation with DAPI. **(E)** Endogenous TBPH shows cytoplasmic expression (arrowheads), as indicated by its co-localisation with membrane-bound GFP. **(F-J)** 5-day old brain of *EB1>mCD8::GFP, TBPH* shows that gain of *TBPH* also leads to cytoplasmic accumulation of TBPH. **(F-H)** Single channels for GFP **(F)**, TBPH **(G)**, and DAPI **(H)** are shown. **(I)** Perinuclear TBPH is clearly seen outside of the DAPI stained nucleus (arrowheads). **(J)** Co-localization of TBPH and the membrane-bound mCD8::GFP indicates cytoplasmic accumulation of overexpressed TBPH (arrowheads). Note: Signal intensity is adjusted for overexpressed TBPH to avoid saturation of the signal. Scale bar: 10µm.

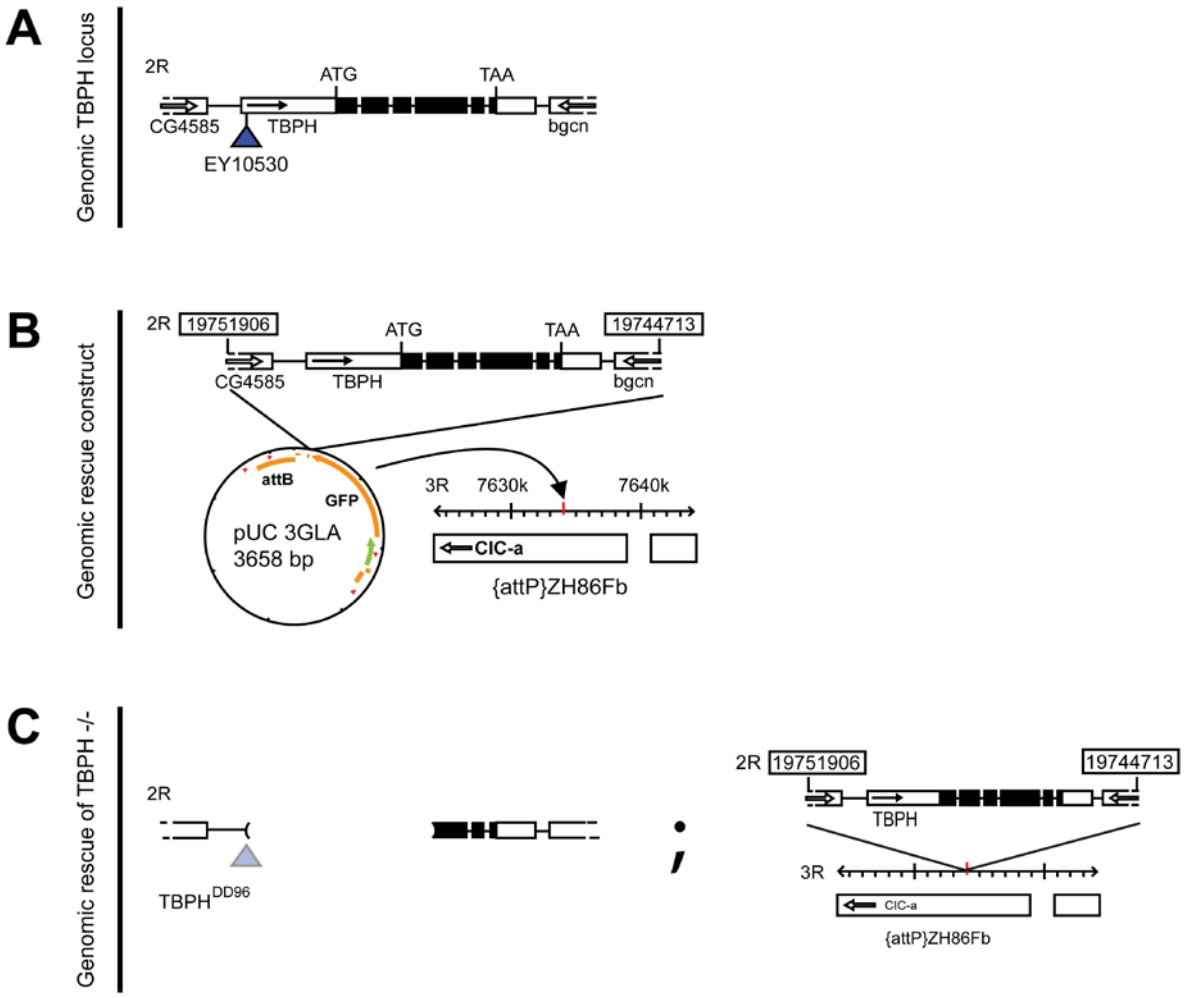

Figure S5. The genomic TBPH locus was used to generated a TBPH rescue construct. (**A**) The TBPH gene is located on the 2R chromosome. Flies containing the EY10530 P-element were used to generate an imprecise excision mutant (C). (**B**) cDNA from the 2R19751906:19744713 region was integrated into a pUC 3GLA plasmid and inserted at position attP 86Fb on the 3R chromosome. (**C**) The genomic TBPH construct was crossed into a *TBPH*^{96} -/- background to generate genomic rescue flies.

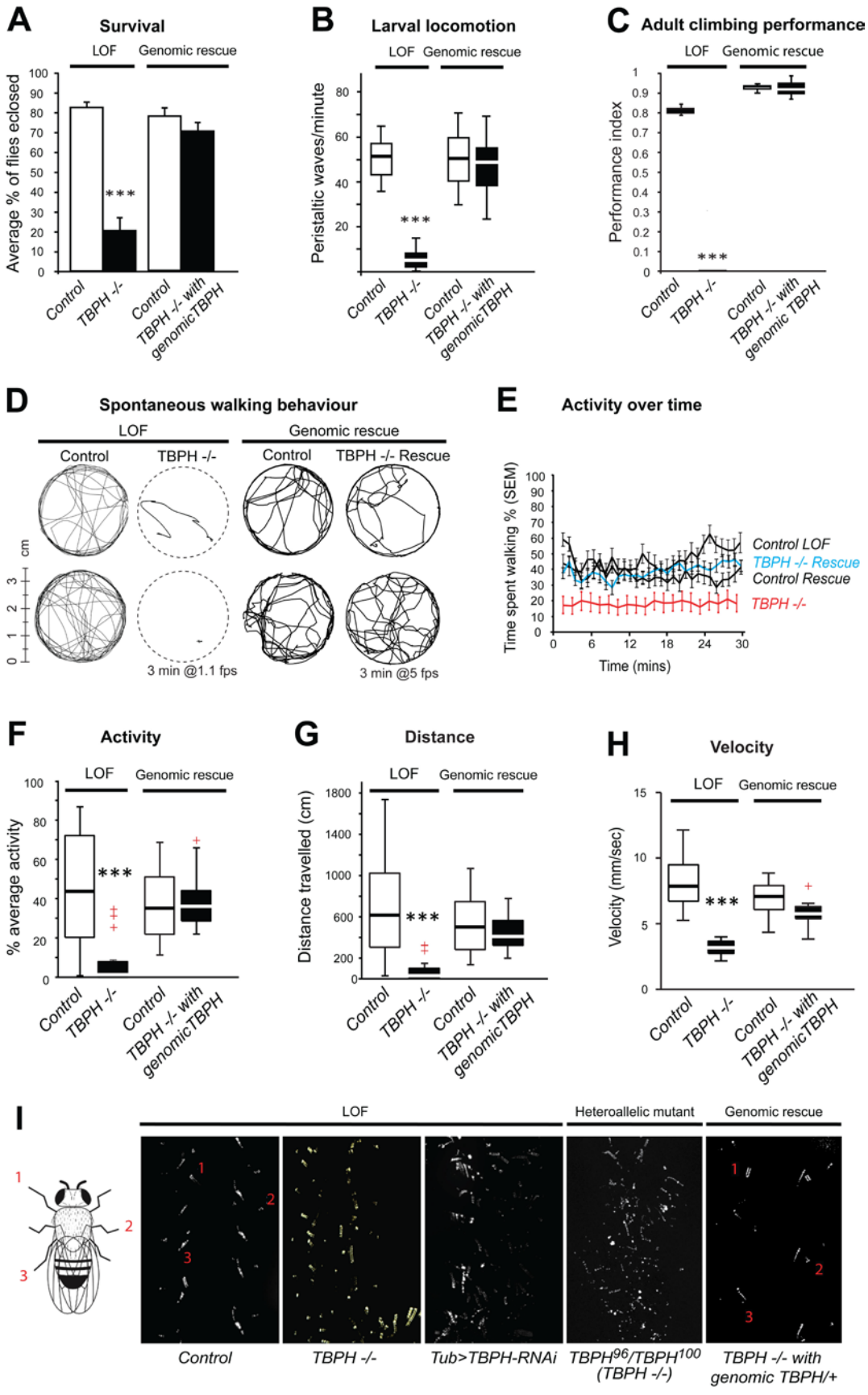

Figure S6. The genomic TBPH construct rescues the TBPH null behaviour phenotypes (**A**) A survival analysis quantified the number of larvae that survived to adulthood. The number of

fully eclosed adults was significantly reduced in loss-of-function (LOF) TBPH null mutants. This eclosion phenotype was rescued by genomic TBPH (genomic rescue, *TBPH^{96}/TBPH^{96};genomicTBPH/genomicTBPH*). (**B**) TBPH LOF shows impaired larval locomotion with a reduction in the number of peristaltic waves per minute, which is rescued by the genomic TBPH construct. (**C**) TBPH LOF adults also show poor climbing performance in a startle-induced climbing assay. This phenotype is fully recued by the genomic TBPH construct. In all cases (a-c), *w^{1118}* served as a control for both LOF and the genomic rescue. (**D**) Representative walking tracks of both TBPH null mutants and the genomic rescue over 3 minutes. Adult flies were allowed to freely walk in a circle arena. (**E-H**) TBPH LOF shows a reduction in walking activity over time, activity and total distance travelled compared to the control (*Oregon R).* All aspects of the walking phenotype were rescued by the genomic TBPH construct. In all cases (D-H), *Oregon R* served as LOF control, and *w^{1118}* as the genomic rescue control. (**I**) TBPH LOF genotypes (*TBPH -/-* and *Tub>TBPH-IR*) display a disturbed tripod gait**.** Left cartoon shows tripod gait with left foreleg (1), right middle leg (2), and left hind leg (3). Control flies (*w^{1118}*) walk in a stereotyped alternating tripod gait pattern. This pattern is disrupted in *TBPH^{DD96}* null mutants (*TBPH-/-*), ubiquitous RNAi-mediated TBPH knockdown flies (*Tub>TBPH-RNAi*) and heteroallelic TBPH mutant flies (*TBPH^{96}/TBPH^{100} -/-*) flies. This tripod gait phenotype is rescued by the genomic TBPH construct. A, E, mean and SEM are indicated. B-C, F-H, box-plots indicate the median, upper and lower quartiles (box); whiskers contain data 1.5x the interquartile range; + indicates a data point within 3x the interquartile range (outliers). ***=P<0.001.

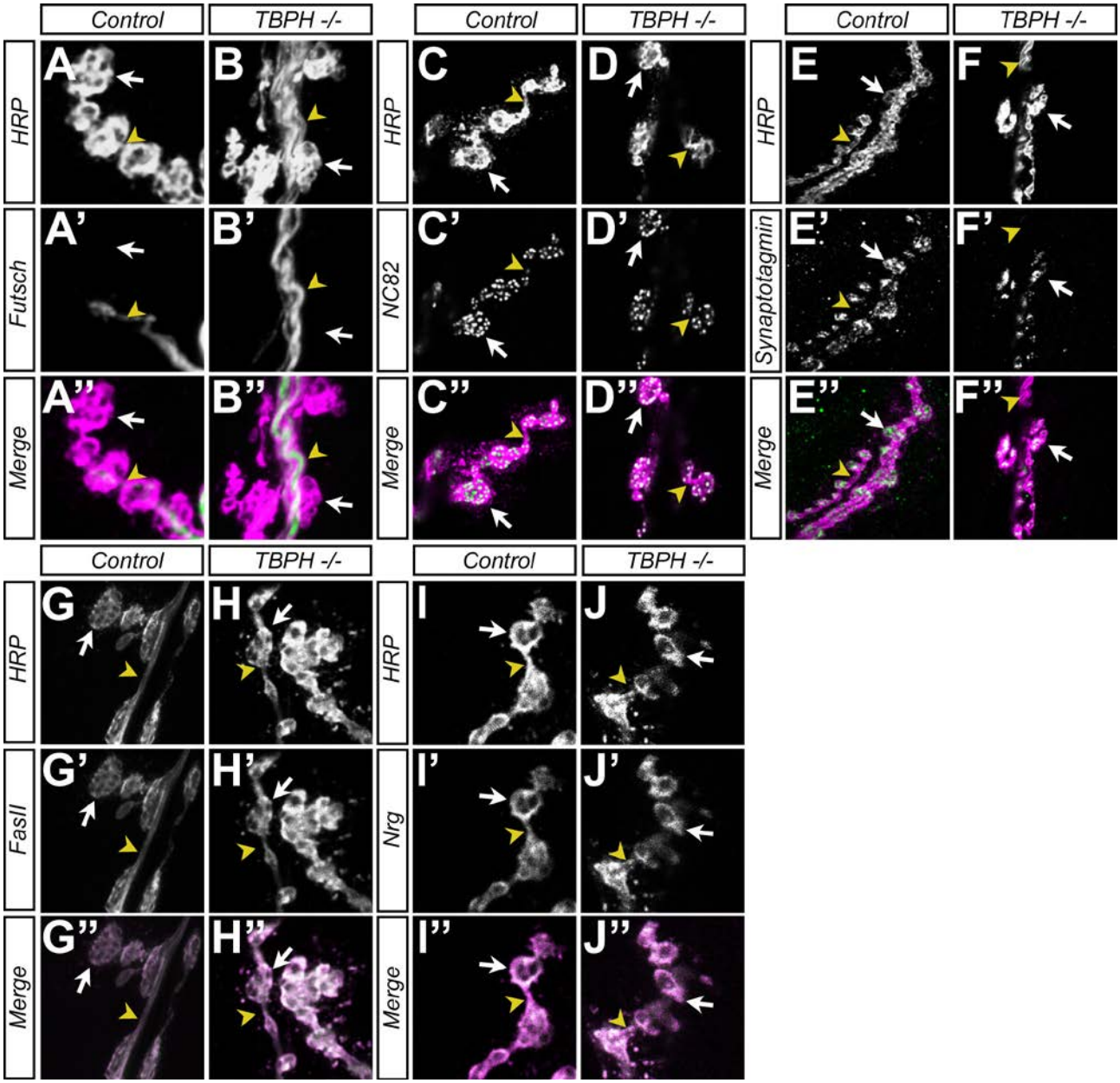

Figure S7. Loss of TBPH does not alter synapse morphology or localization of synaptic proteins at the larval NMJ. A synaptic protein localization analysis was carried out at the neuromuscular junction (NMJ) of muscle group 6/7 of abdominal segment II in control (w^{1118}) and wandering third instar larvae of *TBPH-/-* loss of function mutants. (**A-B''**) The cytoskeletal protein futsch is present in the NMJ axons of both w^{1118} and *TBPH -/-* larvae (yellow arrowhead, however, it is not strongly visualized in the boutons (white arrow) of either genotype. (**C-D''**) Active zone marker NC82 shows punctate expression in the boutons (white arrow) but not the axons for both w^{1118} and *TBPH -/-* larvae (yellow arrowhead). (**E-F''**) Synaptotagmin is clustered in the boutons (white arrow), but not the axons (yellow arrowhead) of both w^{1118} and *TBPH -/-* larvae. (**G-J''**) FasII and Nrg show normal axonal (yellow arrowhead) and bouton (white arrow) expression in both w^{1118} and *TBPH -/-* larvae. All images are single z-slices taken in 1.5µm steps.

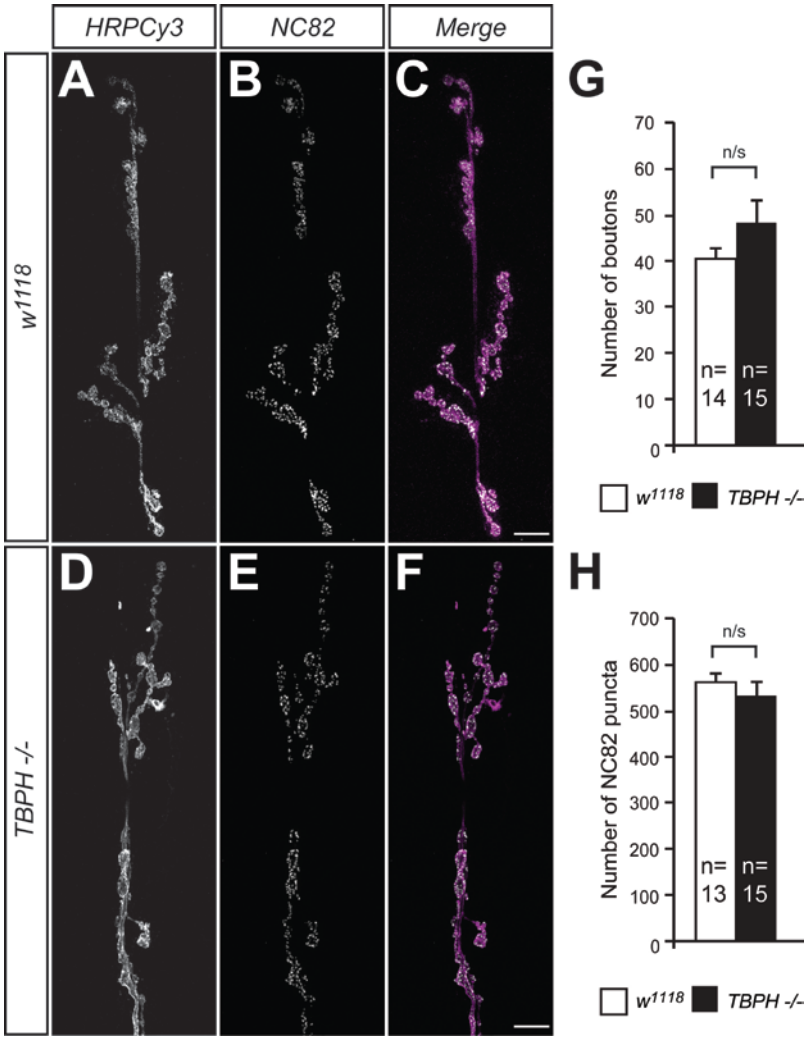

Figure S8. There is no alteration in bouton number or active zone number in TBPH LOF mutants. (**A-C**) The NMJ of w^{1118} wandering L3 larvae, at muscle group 6/7, segment A3 was visualized with HRPCy3 (A), and the active zones identified using the anti-Bruchpilot antibody NC82 (B). (**D-F**) The NMJ of *TBPH -/-* wandering L3 larvae, at muscle group 6/7, segment A3 was visualized with HRPCy3 (D), and the active zones identified using the anti-Bruchpilot antibody NC82 (E). (**G**) There was no difference in the number of boutons counted for each genotype. (**H**) No difference was observed in the number of NC82 punta (active zones) between the genotypes. G, H, mean and SEM are indicated. Scale bar: 10µm.

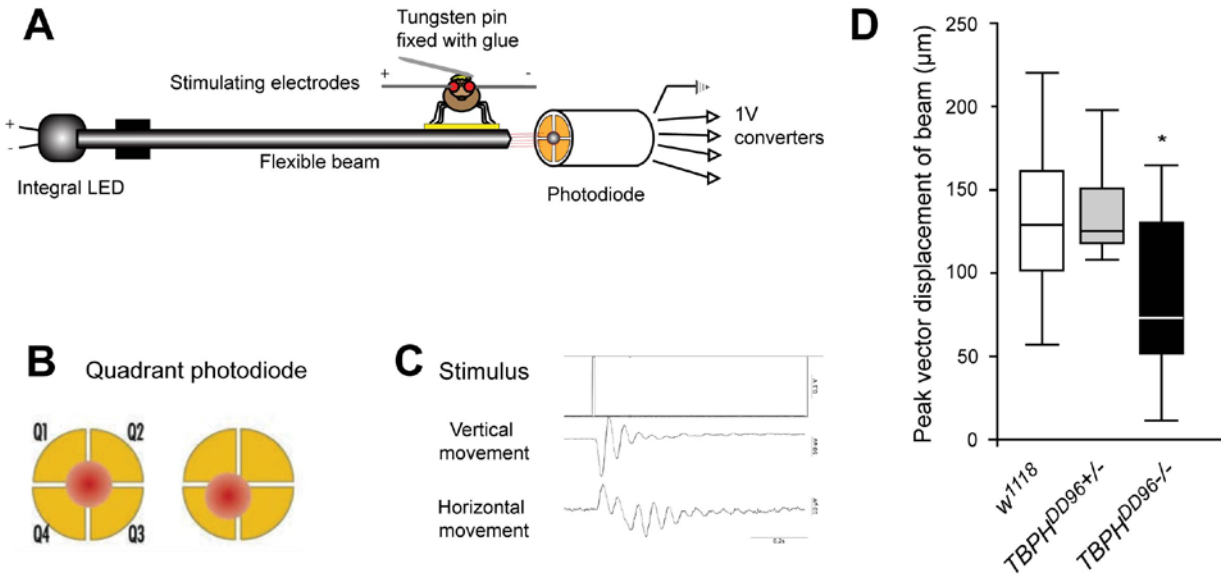

Figure S9. TBPH null mutants show a diminished escape response. The reflex jumping escape response[58] was measured in 5-day-old control (w^{1118} and *TBPH* +/-) and *TBPH* -/- LOF adults. This was carried out by stimulating the Giant Fibre System, which effects a jump reflex from the mesothoracic legs. (**A**) Flies are fixed in place above the ergometer with their legs resting on the jump pad. (**B**) In the resting position, the light travels through the hollow ergometer and sits in the centre of all four detector quadrants. As the fly jumps, the light beam is deflected and the shift in illumination is measured separately by each quadrant. (**C**) In response to a stimulus, both the vertical deflection (jump) and horizontal deflection (direction of jump) are calculated. (**D**) Measuring the vector deflection shows *TBPH* -/- mutants are able to effect an escape jumping response following stimulation of the Giant Fibre System. However, their jump reflex was significantly weaker than that of the heterozygous deletion and w^{1118} control flies. D, ox-plots indicate the median, upper and lower quartiles (box); whiskers contain data 1.5x the interquartile range. (n w^{1118} = 15, n $TBPH^{DD96}$ +/- = 13, n $TBPH^{DD96}$ -/- = 14; *=p<0.05).

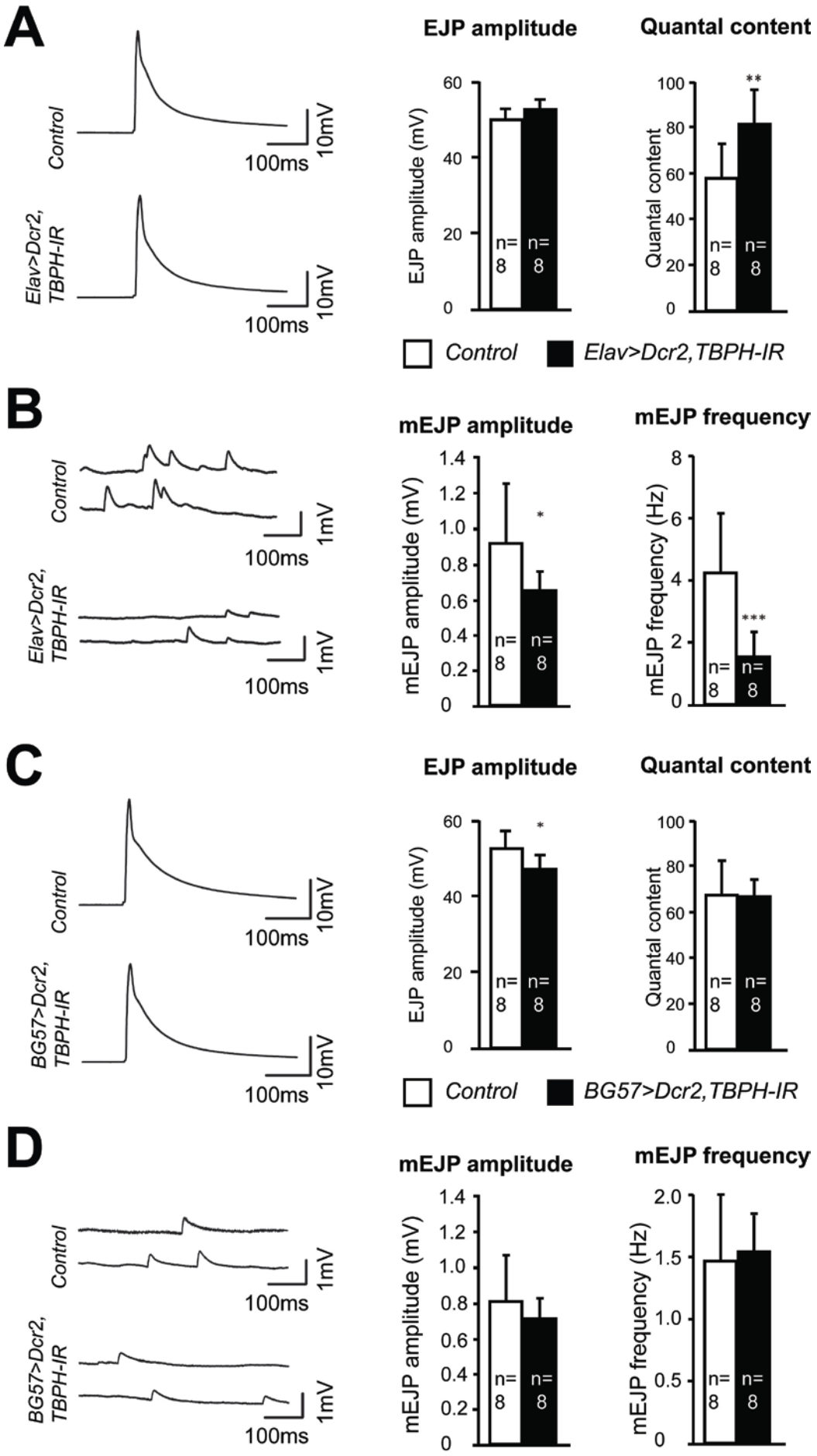
A
Control
10mV
100ms
Elav>Dcr2,
TBPH-IR
10mV
100ms
EJP amplitude
EJP amplitude (mV)
60
40
20
0
n=
8
n=
8
Quantal content
Quantal content
100
80
60
40
20
0
**
n=
8
n=
8
Control
Elav>Dcr2,TBPH-IR
B
Control
1mV
100ms
Elav>Dcr2,
TBPH-IR
1mV
100ms
mEJP amplitude
mEJP amplitude (mV)
1.4
1.2
1.0
0.8
0.6
0.4
0.2
0
*
n=
8
n=
8
mEJP frequency
mEJP frequency (Hz)
8
6
4
2
0
***
n=
8
n=
8
C
Control
10mV
100ms
BG57>Dcr2,
TBPH-IR
10mV
100ms
EJP amplitude
EJP amplitude (mV)
60
40
20
0
*
n=
8
n=
8
Quantal content
Quantal content
100
80
60
40
20
0
n=
8
n=
8
Control
BG57>Dcr2,TBPH-IR
D
Control
1mV
100ms
BG57>Dcr2,
TBPH-IR
1mV
100ms
mEJP amplitude
mEJP amplitude (mV)
1.4
1.2
1.0
0.8
0.6
0.4
0.2
0
n=
8
n=
8
mEJP frequency
mEJP frequency (Hz)
2.0
1.5
1.0
0.5
0
n=
8
n=
8

Figure S10. TBPH-RNAi driven in neurons, but not in muscle, reduces synaptic efficacy at the NMJ. (**A**) Representative excitatory junction potential (EJP) traces are shown for control (*ElavGal4/+;;Dcr2/+*) and for pan-neuronal TBPH knock down (*Elav>TBPH-IR+Dcr2*) wandering 3rd instar larvae. The EJP amplitude for TBPH-RNAi larvae are not significantly different from the control, however, similar to the LOF mutant genotype, quantal content is significantly increased in *Elav>TBPH-IR+Dcr2* larvae. (**B**) Representative traces of spontaneous neurotransmitter release (mEJP) shown for control (*ElavGal4/+;;Dcr2/+*) and for pan-neuronal TBPH knock down (*Elav>TBPH-IR+Dcr2*) wandering 3rd instar larvae. Both the mEJP amplitude and frequency are significantly reduced in *Elav>TBPH-IR+Dcr2* larvae. (**C**) Representative excitatory junction potential (EJP) traces are shown for control (*Dcr2/+;;BG57Gal4/+*) and for muscle-specific TBPH knock down (*BG57>TBPH-IR+Dcr2*) wandering 3rd instar larvae. The EJP amplitude for TBPH-RNAi larvae is significantly reduced in *BG57>TBPH-IR+Dcr2* larvae, however, quantal content is unchanged. (**D**) Representative traces of spontaneous neurotransmitter release (mEJP) shown for control (*Dcr2/+;;BG57Gal4/+)* and for muscle-specific TBPH knock down (*BG57>TBPH-IR+Dcr2*) wandering 3rd instar larvae. Driving TBPH-RNAi with Dcr2 in muscles does not affect the mEJP amplitude or frequency. *=P<0.05, **=P<0.01, ***=P<0.001. Mean and SEM are shown.

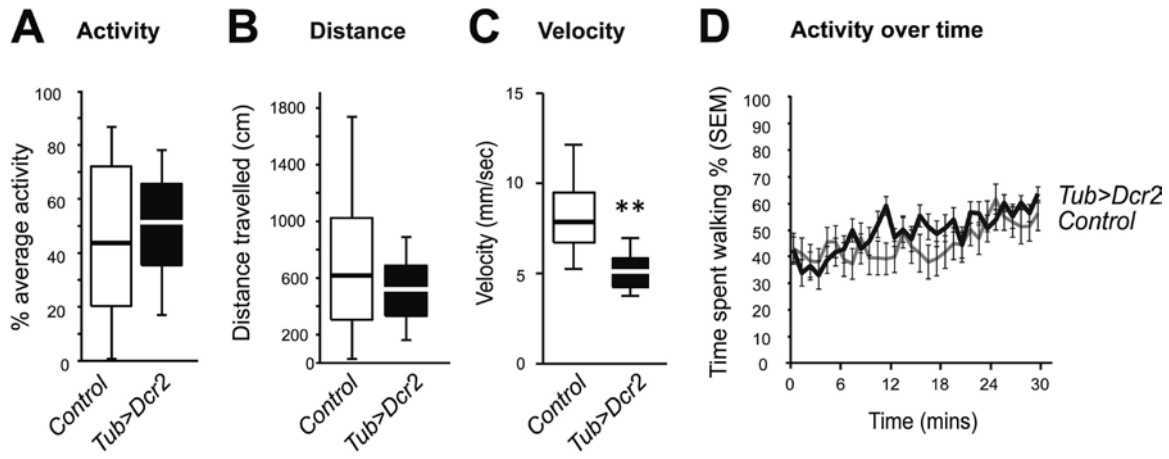

Figure S11. Ubiquitous expression of UAS-Dcr2 alone does not affect the flies' walking ability or distance covered. (**A, B**) The walking activity (A) and distance travelled (B) of flies in unaffected overexpressing Dcr2 with the strong and ubiquitous driver Tubulin-Gal4 (*Tub>Dcr2*). (**C**) The velocity of the *Tub>Dcr2* flies is significantly reduced compared to controls. (**D**) The activity over time of *Tub>Dcr2* is not significantly different to that of the controls. The control genotype is *Oregon R*. A-C, box-plots indicate the median, upper and lower quartiles (box); whiskers contain data 1.5x the interquartile range. D, mean and SEM are indicated. **=P<0.01.

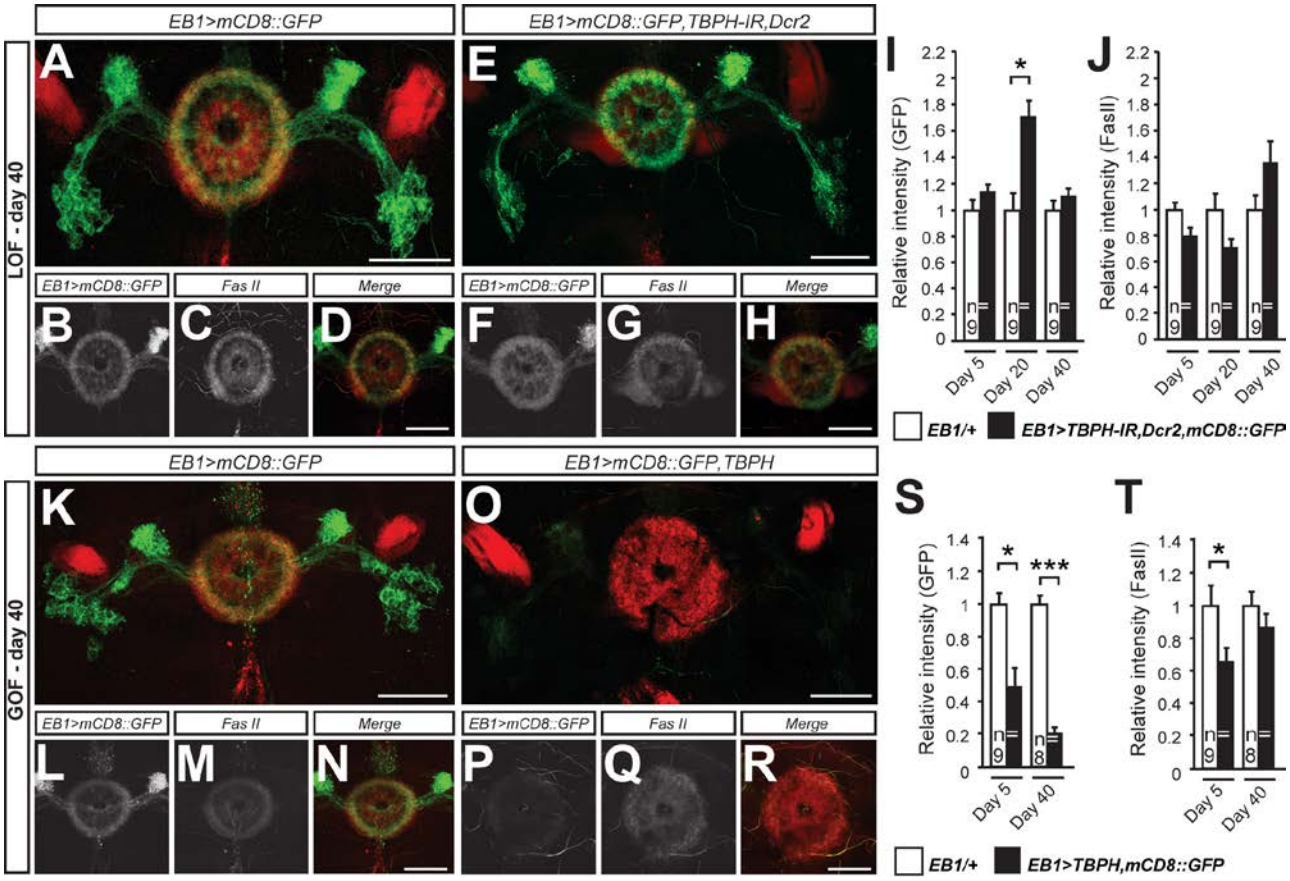

Figure S12. TBPH dysfunction differentially affects synaptic integrity in an age-related manner. (**A-D**) Control flies at day 40 expressing membrane-bound mCD8::GFP in upper motor neurons which visualizes ellipsoid body (EB) ring neuropil that also expressed FasII. (**B, C**) Single channels showing mCD8::GFP (**B**) and FasII (**C**) expression in EB ring neuropil; (**D**) merged image. (**E-H**) Day 40 TBPH LOF flies (*mCD8::GFP, Dcr2, TBPH-IR*) with TBPH-RNAi targeted to upper motor neurons. (**F, G**) Single channels showing mCD8::GFP (**F**) and FasII (**G**) expression in EB ring neuropil; (**H**) merged image. (**I, J**) Quantified relative intensity of mCD8::GFP (**I**) and FasII expression (**J**) in TBPH LOF do not decrease with age when compared to controls. (**K-O**) Control flies at day 40 expressing membrane-bound mCD8::GFP in upper motor neurons and endogenous FasII expression. (**M, N**) Single channels showing mCD8::GFP **(M)** and FasII **(N)** expression in EB ring neuropil; **(O)** merged image. (**L-R**) Day 40 TBPH GOF flies (*EB1>mCD8::GFP, TBPH*) with TBPH overexpression targeted to upper motor neurons. (**P, Q**) Single channels showing mCD8::GFP (**P**) and FasII (**Q**) expression in EB ring neuropil; (**R**) merged image. (**S**) Quantified relative intensity of mCD8::GFP expression in the TBPH GOF flies significantly decreases with age. However, (**T**), quantified relative intensity of FasII expression in TBPH GOF does not decrease with age when compared to controls. *=P<0.05; ***=p<0.001. Scale bars: 50µm

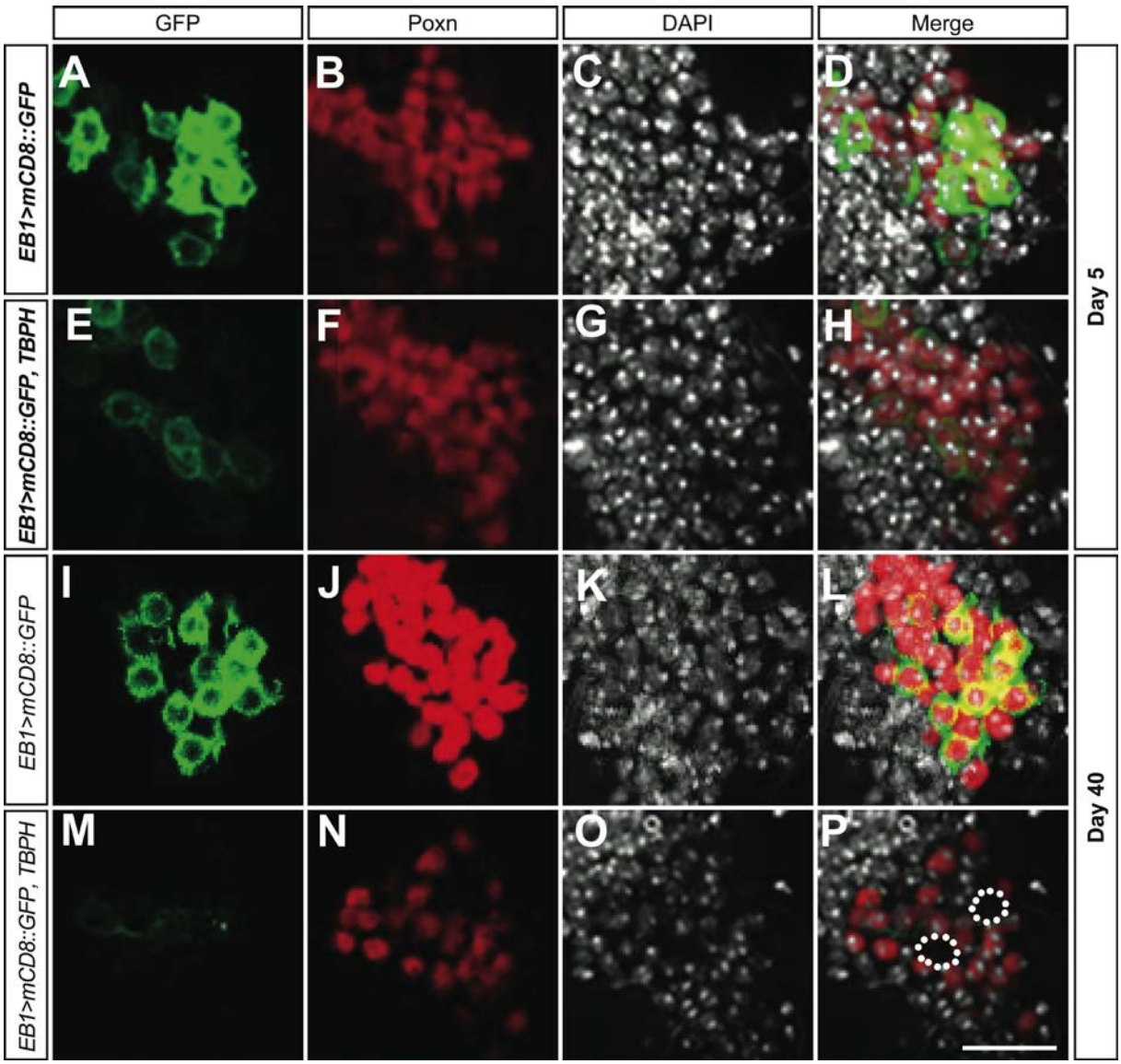

Figure S13. Gain of TBPH causes age-related neurodegeneration. (**A-D**) Control 5-day old *EB1>mCD8::GFP* brain show poxn neuro (Poxn) expression in ellipsoid body neurons of the adult central brain which are considered as upper motor neurons. (**E-H**) Gain of TBPH in 5-day old *EB1>mCD8::GFP,TBPH* brain shows no obvious alteration in the number of Poxn expressing cells. (**I-L**) Control 40-day old *EB1>mCD8::GFP* brain does not show loss of Poxn expressing ellipsoid body neurons. (**M-P**) Gain of TBPH in 40-day old *EB1>mCD8::GFP,TBPH* brain reveals loss of Poxn expressing cells (dotted circle). Scale bar: 10µm

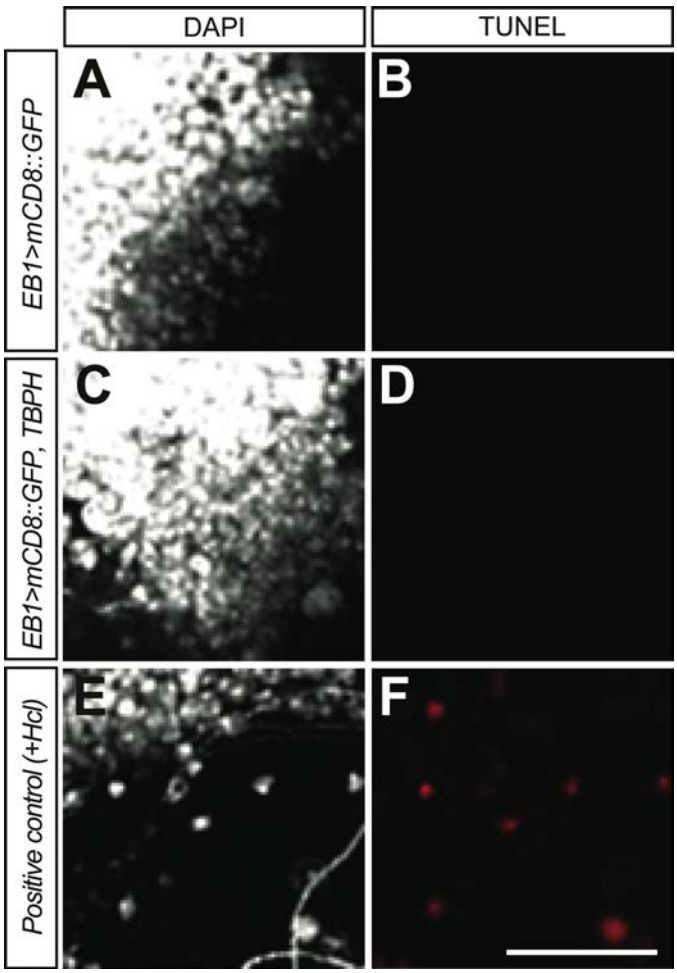

Figure S14. Gain of TBPH neurodegeneration does not occur via apoptosis (**A, B**) Terminal deoxynucleotidyl transferase dUTP nick end labeling (TUNEL) was used to detect DNA fragmentation and apoptotic cell death by labeling the terminal end of nucleic acids. Confocal image of a subset of ellipsoid body neurons in the adult central brain of 40 days old *EB1>mCD8::GFP* flies that were TUNEL labeled; no obvious TUNEL labeling is detectable. (**C, D**) Confocal image of a subset of ellipsoid body neurons in the adult central brain of 40 days old flies that overexpress TBPH (*EB1>mCD8::GFP, TBPH*) and that were TUNEL labeled; no obvious TUNEL labeling is detectable. (**E, F**) Confocal image of a subset of ellipsoid body neurons in the adult central brain of 40 days old control flies that were treated with 2N HCL to induce apoptosis and subsequently TUNEL labeled; TUNEL labeling is detectable in several cells. Scale bar: 20µm.

Table S1. Statistics

Fig.	Test used	Software (version)	Comparison	n	P value	Sig.	Other values
3A	Unpaired t-test	SPSS (15.0)	Survival: *w1118*(control), *TBPH -/-*	3, 3	4.8×10^{-4}	***	t=10.398, df=4
3A	Unpaired t-test	R	Survival: *Elav/+* (control), *ELAV>TBPH*	3, 3	P<0.0001	***	t = 18.9799, df = 2.859
3B	Unpaired t-test (two-tailed)	SPSS (15.0)	Larval locomotion: w^{1118} (control), *TBPH -/-*	30, 30	P<0.0001	***	t=16.178, df=58
3B	Unpaired t-test (two-tailed)	R	Larval locomotion: *ELAV/+* (control), *ELAV>TBPH*	30, 30	P<0.0001	***	t = 8.0726, df = 44.52
3C	Unpaired t-test (two-tailed)	SPSS (15.0)	Climbing: *OregonR* (control), *TBPH -/-*	3,3	1.74×10^{-5}	***	t=24.141, df=4
3C	Unpaired t-test (two-tailed)	R	Climbing: *ELAV/+* (control), *ELAV>TBPH*	3, 3	0.005	**	t = 6.373, df = 3.446
3F	Mann-Whitney U-test, Bonferroni correction	Matlab (7.10.0)	Activity: *OregonR* (control), *TBPH -/-*	24, 18	6.3×10^{-4}	***	
3F	Mann-Whitney U-test, Bonferroni correction	Matlab, GNU Octave	Activity: *EB1>mCD8::GFP* (control), *EB1>mCD8::GFP, TBPH*	18,18	P<0.0001	***	
3G	Mann-Whitney U-test, Bonferroni correction	Matlab (7.10.0)	Distance: *OregonR* (Control), *TBPH-/-*	24, 18	5×10^{-6}	***	
3G	Mann-Whitney U-test, Bonferroni correction	Matlab, GNU Octave	Distance: *EB1>mCD8::GFP* (Control), *EB1>mCD8::GFP,TBPH*	18,18	P<0.0001	***	
3H	Mann-Whitney U-test, Bonferroni correction	Matlab (7.10.0)	Velocity: *OregonR* (control), *TBPH-/-*	24, 18	9.9×10^{-7}	***	
3H	Mann-Whitney U-test, Bonferroni correction	Matlab, GNU Octave	Velocity: *EB1>mCD8::GFP* (control), *EB1>mCD8::GFP, TBPH*	18,18	0.27	n/s	
4A	Unpaired t-test (two-tailed)	GraphPad Prism 5	EJP amplitude: w^{1118}, *TBPH-/-*	10, 9	0.2304	n/s	t=1.244, df=17
4A	Unpaired t-test (two-tailed)	GraphPad Prism 5	EJP amplitude: *ELAV/+*, *ELAV>TBPH*	7,8	0.5606	n/s	t=0.5973, df=13
4A	Unpaired t-test (two-tailed)	GraphPad Prism 5	Quantal content: w^{1118}, *TBPH -/-*	10,9	0.0228	*	t =2.502, df = 17
4A	Unpaired t-test (two-tailed)	GraphPad Prism 5	Quantal content: *ELAV/+*, *ELAV>TBPH*	7,8	0.2758	n/s	t = 1.138, df = 13
4B	Unpaired t-test (two-tailed)	GraphPad Prism 5	mEJP amplitude: w^{1118}, *TBPH -/-*	10,9	0.0089	**	t = 2.951, df = 17
4B	Unpaired t-test (two-tailed)	GraphPad Prism 5	mEJP amplitude: *ELAV/+*, *ELAV>TBPH*	7,8	0.1343	n/s	t = 1.597, df = 13
4B	Unpaired t-test (two-tailed)	GraphPad Prism 5	mEJP frequency:w^{1118}, *TBPH -/-*	10,9	0.0435	*	t = 2.181, df = 17
4B	Unpaired t-test (two-tailed)	GraphPad Prism 5	mEJP frequency: *ELAV/+*, *ELAV>TBPH*	7,8	0.9973	n/s	t = 0.003504, df = 13

4D	ANOVA with Bonferroni post-hoc tests	SPSS (17.0)	Peak-peak ERG response: *TBPH -/-*, w^{1118} (control)	20,19	P=1.0	n/s	
4D	ANOVA with Bonferroni post-hoc tests	SPSS (17.0)	*GMR>UAS-TBPH-RNAi*, *OregonR* (control)	20,20	0.058	n/s	
4E	Sign test, data points above/below regression line	Manual calculation	*TBPH-/-*, regression line	19	0.013	*	□2 =6.1, df=1
4E	Sign test, data points above/below regression line	Manual calculation	*GMR>UAS-TBPH-RNAi*, regression line	20	<0.001	***	□2 =16.2, df=1
4G	ANOVA with Bonferroni post-hoc tests	SPSS (19.0)	*GMR/w^{1118}*, *GMR>TBPH*	9,9	<0.001	***	
5C	Mann-Whitney U-test, Bonferroni correction	Matlab (7.10.0)	Activity: *Dcr2/+;TBPH-IR/+;+*(control), *TBPH-/-*	24, 18	<1.0 x 10^{-17}	***	
5C			Activity: *Dcr2/+;TBPH-IR/+;+* (control), *Dcr2/+;TBPH-IR/+;TubGAL4/+*	24,24	1.0 x 10^{-6}	***	
5C			Activity: *TBPH-/-*, *Dcr2/+;TBPH-IR/+;TubGAL4/+*	18, 24	0.0022	**	
5D	Mann-Whitney U-test, Bonferroni correction	Matlab (7.10.0)	Distance: *Dcr2/+; TBPH-IR/+;* + (control), *TBPH-/-*	24,18	<1.0 x 10^{-7}	***	
5D			Distance: *Dcr2/+; TBPH-IR/+;* + (control), *Dcr2/+; TBPH-IR/+; TubGAL4/+*	24,24	1.0 x 10^{-7}	***	
5D			Distance: *TBPH-/-*, *Dcr2/+; TBPH-IR/+; TubGAL4/+*	18, 24	0.0012	**	
5E	Mann-Whitney U-test, Bonferroni correction	Matlab (7.10.0)	Velocity: *Dcr2/+; TBPH-IR/+;* + (control), *TBPH-/-*	24, 18	2.0 x 10^{-6}	***	
5E			Velocity: *Dcr2/+; TBPH-IR/+;* + (control), *Dcr2/+; TBPH-IR/+; TubGAL4/+*	24, 24	<1.0 x 10^{-7}	***	
5E			Velocity: *TBPH -/-*, *Dcr2/+; TBPH-IR/+; TubGAL4/+*	18, 24	P=0.0310	*	
5G	Mann-Whitney U-test, Bonferroni correction	Matlab (7.10.0)	Activity: *Dcr2/+; TBPH-IR/+;+* (control), *TBPH -/-*	24, 18	<1.0 x 10^{-7}	***	
5G			Activity: *Dcr2/+; TBPH-IR/+;+* (control), *ELAV>TBPH-IR, Dcr2*	24, 24	<1.0 x 10^{-7}	***	
5G			Activity: *Dcr2/+; TBPH-IR/+;+* (control), *EB1>TBPH-IR, Dcr2*	24,24	<1.0 x 10^{-7}	***	
5G			Activity: *TBPH -/-*, *ELAV>TBPH-IR, Dcr2*	18, 24	3.8 x 10^{-4}	***	
5G			Activity: *TBPH -/-*, *EB1>TBPH-IR, Dcr2*	18, 24	4.1 x 10^{-5}	***	
5H	Mann-Whitney U-test, Bonferroni correction	Matlab (7.10.0)	Distance: *Dcr2/+; TBPH-IR/+;+* (control), *TBPH -/-*	24, 18	<1.0 x 10-7	***	
5H			Distance: *Dcr2/+; TBPH-IR/+;+* (control), *ELAV>TBPH-IR, Dcr2*	24,24	1.0 x 10-6	***	

5H			Distance: *Dcr2/+; TBPH-IR/+;+* (control), *EB1>TBPH-IR, Dcr2*	24,24	<1.0 x 10-7	***	
5H			Distance: *TBPH -/-*, *ELAV>TBPH-IR, Dcr2*	18, 24	8.4 x 10-5	***	
5H			Distance: *TBPH -/-*, *EB1>TBPH-IR, Dcr2*	18, 24	4.7 x 10-5	***	
5I	Mann-Whitney U-test, Bonferroni correction	Matlab (7.10.0)	Velocity: *Dcr2/+; TBPH-IR/+;+* (control), *TBPH -/-*	24, 18	2.0 x 10-6	***	
5I			Velocity: *Dcr2/+; TBPH-IR/+;+* (control), *ELAV>TBPH-IR, Dcr2*	24,24	2.88 x 10-4	***	
5I			Velocity: *Dcr2/+; TBPH-IR/+;+* (control), *EB1>TBPH-IR, Dcr2*	24, 24	<1.0 x 10-7	***	
5I			Velocity: *TBPH -/-*, *ELAV>TBPH-IR, Dcr2*	18, 24	3.0 x 10-6	***	
5I			Velocity: *TBPH -/-*, *EB1>TBPH-IR, Dcr2*	18, 24	2.1 x 10-5	***	
6G	Unpaired t-test (two-tailed)	SPSS (20.0)	DenMark intensity: *EB1>Syt::GFP, DenMark* (control), *EB1>Syt::GFP, DenMark, TBPH-IR+Dcr2*	8, 9	0.000329	***	t=4.627, df=15
6H	Unpaired t-test (two-tailed)	SPSS (20.0)	Syt::GFP intensity: *EB1>Syt::GFP, DenMark* (control), *EB1>Syt::GFP, DenMark, TBPH*	8, 9	0.015	*	t=2.762, df=14
6O	Unpaired t-test (two-tailed)	R	DenMark intensity: *EB1>Syt::GFP, DenMark* (control), *EB1>Syt::GFP, DenMark, TBPH-IR+Dcr2*	10, 12	4.748 x 10^{-5}	***	t=5.266, df=18.559
6P	Unpaired t-test (two-tailed)	R	Syt::GFP intensity: *EB1>Syt::GFP, DenMark* (control), *EB1>Syt::GFP, DenMark, TBPH*	9,8	0.04	*	t=5.266, df=12.414
7G	2-way ANOVA	ANOVA4 on the web	Cell number: *EB1>mCD8::GFP* (control), *EB1>mCD8::GFP, TBPH-IR, Dcr2* [day5, 20, 40]	18,18,18,18,17	0.0011	**	F=11.215
7G					Age <0.0001	***	F=14.269
7G	Ryan's method	ANOVA4 on the web	Cell number (day5): *EB1>mCD8::GFP* (control), *EB1>mCD8::GFP, TBPH-IR, Dcr2*	18,18	0.4269	n/s	
7G			Cell number (day40): *EB1>mCD8::GFP* (control), *EB1>mCD8::GFP, TBPH-IR, Dcr2*	18,17	<0.0001	***	
7G			Cell number (day50): *EB1>mCD8::GFP (control), EB1>mCD8::GFP, TBPH-IR, Dcr2*	18,18	<0.0001	***	

7G			Cell number: *EB1>mCD8::GFP* (control, day5), *EB1>mCD8::GFP* (control, day20)	18,18	0.0025087	**	
7G			Cell number: *EB1>mCD8::GFP, TBPH-IR, Dcr2* (day5), *EB1>mCD8::GFP, TBPH-IR, Dcr2* (day40)	18,17	P<0.0000001	***	
7G			Cell number: *EB1>mCD8::GFP, TBPH-IR, Dcr2* (day5), *EB1>mCD8::GFP, TBPH-IR, Dcr2* (day20)	18,18	0.1521008	n/s	
7G			Cell number: *EB1>mCD8::GFP, TBPH-IR, Dcr2* (day20), *EB1>mCD8::GFP, TBPH-IR, Dcr2* (day40)	18,17	0.0000056	***	
7N	2-way ANOVA	ANOVA4 on the web	Cell number: *EB1>mCD8::GFP* (control), *EB1>mCD8::GFP, TBPH* [day5, 40, 60]	10, 10, 10, 10, 8, 10	Genotype P<0.0001	***	F=66.004
7N					Age P=0.0003	***	F=9.584
7N	Ryan's method	ANOVA4 on the web	Cell number (day5): *EB1>mCD8::GFP* (control), *EB1>mCD8::GFP, TBPH*	10, 10	0.6266	n/s	
7N			Cell number (day40): *EB1>mCD8::GFP* (control), *EB1>mCD8::GFP, TBPH*	10, 10	P<0.0001	***	
7N			Cell number (day60): *EB1>mCD8::GFP (control), EB1>mCD8::GFP, TBPH*	8, 10	P<0.0001	***	
7N			Cell number: *EB1>mCD8::GFP, TBPH* (day5), *EB1>mCD8::GFP, TBPH* (day60)	10, 10	P<0.0000001	***	
7N			Cell number: *EB1>mCD8::GFP, TBPH* (day5), *EB1>mCD8::GFP, TBPH* (day40)	10, 10	P=0.0000547	***	
7N			Cell number: *EB1>mCD8::GFP, TBPH* (day40), *EB1>mCD8::GFP, TBPH* (day60)	10, 10	P=0.0201187	*	
8B	One-way ANOVA	ANOVA4 on the web	Endogenous *TBPH* level: *GMR/+*, *GMR>Flag-TBPH-HA*(773II), *GMR>Flag-TBPH-HA*(774III), *GMR>RFP-TBPH*	4,4, 4,4	0.595	n/s	F=0.655
S6F	Mann-Whitney U-test, Bonferroni correction	Matlab (7.10.0)	Activity: *w1118* (control), TBPH-/-(96);genomicTBPH	24, 24	0.927676	n/s	
S6G			Distance: *w1118* (control), TBPH-/-(96);genomicTBPH	24, 24	0.995893	n/s	

S6H			Velocity: *w1118* (control), TBPH-/-(96);genomicTBPH	24, 24	0.116381	n/s	
S8G	Unpaired t-test (two-tailed)	SPSS (20.0)	Bouton number: *w1118* (control), TBPH-/-	14, 15	0.122	n/s	t=-1.597, df=27
S8H	Unpaired t-test (two-tailed)	SPSS (20.0)	NC82 puncta: *w1118* (control), TBPH-/-	14, 15	0.455	n/s	t=.759, df=27
S9D	One-way ANOVA	SPSS (15.0)	Escape response: w^{1118}, *TBPH +/-*, *TBPH -/-*	15,13,14	0.011	*	F=5.055
S9D	Tukey's HSD	SPSS (15.0)	w^{1118}, *TBPH -/-*	15,14	0.034	*	
S9D			*TBPH +/-*, *TBPH -/-*	13, 14	0.017	*	
S10 A	Unpaired t-test (two-tailed)	GraphPad Prism 5	EJP amplitude: Elav_Control, Elav>TBPH_RNAi_RNAi	9,9	0.2926	n/s	t = 1.088 df = 16
S10 A	Unpaired t-test (two-tailed)	GraphPad Prism 5	Quantal content: Elav_Control, Elav>TBPH_RNAi	9,9	0.0042	**	t = 3.332 df = 16
S10B	Unpaired t-test (two-tailed)	GraphPad Prism 5	mEJP amplitude: Elav_Control, Elav>TBPH_RNAi	9,9	0.0291	*	t = 2.397 df = 16
S10B	Unpaired t-test (two-tailed)	GraphPad Prism 5	mEJP frequency: Elav_Control, Elav>TBPH_RNAi	9,9	0.0007	***	t = 4.180 df = 16
S10C	Unpaired t-test (two-tailed)	GraphPad Prism 5	EJP amplitude: BG57_Control, BG57>TBPH_RNAi	9,9	0.0245	*	t = 2.483 df = 16
S10C	Unpaired t-test (two-tailed)	GraphPad Prism 5	Quantal content: BG57_Control, BG57>TBPH_RNAi	9,9	0.8020	n/s	t = 0.2550 df = 16
S10 D	Unpaired t-test (two-tailed)	GraphPad Prism 5	mEJP amplitude: BG57_Control, BG57>TBPH_RNAi	9,9	0.3118	n/s	t = 1.044 df = 16
S10 D	Unpaired t-test (two-tailed)	GraphPad Prism 5	mEJP frequency: BG57_Control, *BG57>TBPH_RNAi*	9,9	0.7800	n/s	t = 0.2841 df = 16
S11 A	Mann-Whitney U-test, Bonferroni correction	Matlab (7.10.0)	Activity: OregonR (control), *Tub>Dcr2*	24, 24	0.9937	n/s	
S11B	Mann-Whitney U-test, Bonferroni correction	Matlab (7.10.0)	Distance: OregonR (control), *Tub>Dcr2*	24, 24	0.8133	n/s	
S11C	Mann-Whitney U-test, Bonferroni correction	Matlab (7.10.0)	Velocity: OregonR (control), *Tub>Dcr2*	24, 24	0.0022	n/s	
S12I	Unpaired t-test (two-tailed)	SPSS (15.0)	GFP intensity (LOF) day 5: *EB1>mCD8::GFP (control), EB1>mCD8::GFP, TBPH-IR+Dcr2*	9, 9	0.1670	n/s	t=-1.448 df=16
S12I	Unpaired t-test (two-tailed)	SPSS (15.0)	GFP intensity (LOF) day 20: *EB1>mCD8::GFP (control), EB1>mCD8::GFP, TBPH-IR+Dcr2*	9, 9	0.001129	*	t=-4.013 df=15
S12I	Unpaired t-test (two-tailed)	SPSS (15.0)	GFP intensity (LOF) day 40: *EB1>mCD8::GFP (control), EB1>mCD8::GFP, TBPH-IR+Dcr2*	9, 9	0.224	n/s	t=-1.264 df=16

S12J	Unpaired t-test (two-tailed)	SPSS (15.0)	FasII intensity (LOF) day 5: *EB1>mCD8::GFP (control), EB1>mCD8::GFP, TBPH-IR+Dcr2*	9, 9	0.19	n/s	t=-2.614, df=16
S12J	Unpaired t-test (two-tailed)	SPSS (15.0)	FasII intensity (LOF) day 20: *EB1>mCD8::GFP (control), EB1>mCD8::GFP, TBPH-IR+Dcr2*	9, 9	0.23	n/s	t=-1.576, df=16
S12J	Unpaired t-test (two-tailed)	SPSS (15.0)	FasII intensity (LOF) day 40: *EB1>mCD8::GFP (control), EB1>mCD8::GFP, TBPH-IR+Dcr2*	9, 9	0.069	n/s	t=-1.948, df=16
S12S	Unpaired t-test (two-tailed)	SPSS (15.0)	GFP intensity (GOF) day5: *EB1>mCD8::GFP* (control), *EB1>mCD8::GFP, TBPH*	9, 9	0.0100	*	t=3.908, df=15
S12S	Unpaired t-test (two-tailed)	SPSS (15.0)	GFP intensity (GOF) day40: *EB1>mCD8::GFP* (control), *EB1>mCD8::GFP, TBPH*	8, 8	3.9 x 10-10	***	t=15.304, df=14
S12T	Unpaired t-test (two-tailed)	SPSS (15.0)	FasII intensity (GOF) day5: *EB1>mCD8::GFP* (control), *EB1>mCD8::GFP, TBPH*	9, 9	0.023	*	t=-2.528, df=15
S12T	Unpaired t-test (two-tailed)	SPSS (15.0)	FasII intensity (GOF) day40: *EB1>mCD8::GFP* (control), *EB1>mCD8::GFP, TBPH*	8, 8	0.132	n/s	t=1.595, df=14